Accelerating Interference-based QoS Analysis of Vehicular Ad Hoc Networks for BSM Safety Applications: Parallel Numerical Solutions and Simulations

Jing Zhao[1,3][a], Hao Zhou[1], YanBin Wang[2], HuaLin Lu[4], Zhijuan Li[4][b] and XiaoMin Ma[5]

[1]*School of Software Technology, Dalian University of Technology, Dalian 116024, China*

[2]*Department of Industrial Engineering, Harbin Institute of Technology, Harbin 150001, China*

[3]*Cyberspace Security Research Center, Peng Cheng Laboratory, Shenzhen 518052, China*

[4]*Department of Computer Science and Technology, Harbin Engineering University, Harbin 150001, China*

[5]*College of Science and Engineering, Oral Roberts University, Tulsa, OK 74171, U.S.A.*

Keywords: Vehicle-to-Vehicle Communication, MPI, Signal-to-Interference-to-Noise, Capacity, QoS.

Abstract: Vehicular Ad-hoc Networks (VANETs) have been proposed and investigated for road safety applications. Many safety applications are enabled by broadcasting basic safety message (BSM) periodically. Whether the current IEEE802.11p communication system can meet the stringent quality of service (QoS) requirement for safety applications is under discussion. Many analytical and simulation models have been proposed to study the reliability of DSRC (Dedicated Short Range Communication) IEEE802.11p broadcast services. However, most analyses assume a deterministic communication range, which is unpractical. In this paper, we propose an analytical model based on signal-to-interference-plus-noise ratio (SINR) to study of QoS and capacity of VANET for BSM based safety applications. The analytical model considers the context of the more practical vehicular communication environment: BSM broadcast, asynchronous timing between hidden terminals, Nakagami channel fading, and Non-Homogeneous Poisson Process vehicle distribution. For the proposed model, the computation complexity of QoS and capacity metrics by numerical solutions is so high that the computation time is intolerable. Thus the efficient numerical way together with a parallel approach is needed to evaluate these metrics. The Monte Carlo integration and MPI (Message Passing Interface) method are applied for accelerating the computing process. The analysis of QoS metrics are validated by NS2 simulation.

1 INTRODUCTION

Intelligent Transportation System (ITS) (Andrisano et al., 2000) is moving in the direction of safe and comfortable driving. Vehicular ad hoc network (VANET) plays an important role in ITS. Among the many applications supported by VANET, safety application is the most critical. Many safety applications are accomplished by broadcasting basic safety message (BSM), and these safety applications have strict quality of service (QoS) requirements. Research on whether the vehicle communication system based on DSRC can meet the QoS requirements of safety applications is also under way. At present, many analytical models along with extensive simulations have been proposed to study the performance and reliability of DSRC IEEE 802.11p broadcast traffic in one-dimensional (Luong et al., 2017; Bazzi et al., 2018; Ma et al., 2013b; Yin et al., 2013; Yao et al., 2013; Ma et al., 2021) and two-dimensional intersections (Ma et al., 2013a; Steinmetz et al., 2015; Ma et al., 2016) VANET. However, the current analysis of VANET QoS and capacity mostly assumes that the communication range is deterministic, and the communication range and hidden terminals are important factors affecting packet reception, which is impractical. In addition, for the purpose of analytical tractability, many impractical assumptions are made, such as the exponential vehicle distribution (Ma et al., 2011; Hafeez et al., 2013; Yin et al., 2013; Ma et al., 2013b) and the Raleigh fading channel model considering path loss (Ye et al., 2011), etc.

[a] https://orcid.org/0000-0001-8529-3399

[b] https://orcid.org/0000-0002-2162-5654

Zhao, J., Zhou, H., Wang, Y., Lu, H., Li, Z. and Ma, X.
Accelerating Interference-based QoS Analysis of Vehicular Ad Hoc Networks for BSM Safety Applications: Parallel Numerical Solutions and Simulations.
DOI: 10.5220/0010472306000610
In *Proceedings of the 7th International Conference on Vehicle Technology and Intelligent Transport Systems (VEHITS 2021)*, pages 600-610
ISBN: 978-989-758-513-5

A few analytic models have been used to evaluate the reliability metrics of PRP(Packet reception probability)/PRR(Packet reception ratio) of 1-D broadcast mobile ad-hoc networks (MANETs) (Ma et al., 2011; Ye et al., 2011; Yin et al., 2013; Hassan et al., 2011; Hafeez et al., 2013; Ma et al., 2013b; Tong et al., 2016; Yao et al., 2013). These kinds of analytical approaches take the impact of the hidden terminal problem, the fading channel, and the channel access protocol into consideration, investigate the performance of VANET at different densities, different receiving distances, and different channel model (such as Nakagami-*m* Fading, Weibull Fading, Rayleigh Fading and Rician Fading). However, few models could provide the practical as well as a viable approach to estimate the actual VANET capacity. Several studies for VANET capacity using scaling-law based method can only give per-node capacity scales in asymptotically large wireless networks (Wang et al., 2015; Lu and Shen, 2014), which cannot be easily applied to actual capacity estimation.

Most recently, a new interference-based capacity model was proposed for VANET safety message broadcast scenario (Ni et al., 2015; Ma et al., 2017). The model approached the capacity analysis of one-dimensional (1-D) VANET safety message broadcast under *Nakagami* fading channel through the derivation of SINR distribution after making reasonable approximations. This model enables the evaluation of VANET capacity for safety applications in a more practical way.

The SINR is the ratio of the strength of the received useful signal to the strength of the received interference signal (noise and interference). BER (bit error rate) represents the probability that a bit is misinterpreted at a receiver due to the propagation process (Yao et al., 2014; Molisch, 2012), which is the function of the SINR. SINR threshold is defined as the value whose mapping BER is small enough(usually 10^{-5}) for the tolerable transmission error. The actual physical communication system such as a real radio hardware USRP (Gotsis et al., 2017), or the simulation components for DSRC such as popular tools NS2 (Chen et al., 2007), NS3 (Eckermann et al., 2019; Shaban et al., 2020), and Matlab (Gotsis et al., 2017; Bazzi et al., 2019) employ the SINR threshold communication mechanism to receive the data packet. Accordingly, estimating entire network capacity or evaluating the performance of VANET Based on SINR distribution could be obtained. Therefore, the SINR based modeling approach to analyze the QoS VANET not only represent the actual communication system features, but also establish the quantization standard such as Capacity and QoS.

Although the SINR based modeling approach for VANET has some advantages compared with the deterministic distance based modeling approach, the computation complexity of the SINR based far exceeds the deterministic distance approach. Message Passing Interface (MPI) (Gropp et al., 1996) is a message-passing standard that is widely used to solve scientific computing problems on parallel computers. It provides a rich collection of interfaces for communication between processes. MPI supports point-to-point communication and collective communication. Thanks to the parallel model MPI, the complex high dimensional integrations could be transformed into solvable problem. VANET QoS metrics have no efficent numerical solutions based on SINR model(Ma et al., 2017), since it needs efforts to find an efficient numerical way to evaluate those metrics. To accelerate the computing process, there are two directions for optimization, reducing integral sampling points and computing integrand in parallel. For reducingg integral sampling points, several delicate approaches can be adopted, such as Monte Carlo integration(Morokoff and Caflisch, 1995), Sparse grids(Gerstner and Griebel, 1998), Bayesian quadrature(Gunter et al., 2014), etc. Some of them such as Bayesian quadrature is hard to parallelism since each iteration of algorithm is related to the last iteration before. For computing integrands in parallel, many research try to compute integrands in parallel by GPU (Arumugam et al., 2013; Zong et al., 2019) or FPGA (Razak et al., 2017), which is significantly faster than compute by CPU. The hardware feature of GPU and FPGA make them can only do the simple evaluation, while the integrands of model by SINR is too complex to implement on them. Therefore, in this paper, we choose Monte Carlo integration as well as MPI method to accelerate computing process.

In this paper, to build a firm and complete framework of the SINR based approach to the capacity and QoS of VANET for safety message broadcast, we come up with a new systematic approach to derivation of the transmission probability and the SINR distribution in the context of BSM safety applications with more general vehicle distribution. The new approach considers the impact of IEEE 802.11p MAC channel access and asynchronous timing between hidden terminals. Then the SINR based analysis is further extended to the analysis of QoS metrics for the safety applications.

Main Contributions of this paper are summarized as follows:

- An analytical model based on SINR is built with Non-Homogeneous Poisson Process (NHPP) node distribution in 1-D, unsaturated message generation, Nakagami channel fading with path loss, and impact of hidden terminal.

- The new model derives the SINR distribution through MPI Monte Carlo programming model, which transform the complex numerical computation to an actual solvable problem.
- Simulations and experiments are proposed for the analysis of validity, computational efforts, accuracy of the model by SINR.

2 PROBLEM FORMULATION AND ASSUMPTIONS

2.1 Problem Formulation

Given a highway vehicular environment on which all vehicles are equipped with IEEE 802.11p DSRC wireless communication capability, each vehicle broadcasts BSM containing measured mobility information to all surrounding vehicles in its transmission range periodically with message generation rate λ, and receives the BSMs from the surrounding vehicles. In this way, awareness range of drivers can be extended and more accidents can be avoided (Schmidt-Eisenlohr, 2010). The safety-related message broadcast requires high reliability and performance. However, the quality of service (QoS) is degraded by message collisions and fading communication channel. We are concerned about if the current DSRC system, under certain vehicular environment, is able to provide the broadcast service with guaranteed QoSs for all selected safety applications. In order to evaluate the system in this regard, several QoS metrics and capacity need to be evaluated: 1) Message (packet) delivery probability defined as the probability that a receiver successfully decodes the message (packet) from a source node with a distance. 2) Packet (message) reception ratio defined as the percentage of receivers in a range that are free from transmission errors once a broadcast message is sent out. 3) Link capacity defined as the maximum message (packet) transmission rate between two nodes in the communication channel.

2.2 Assumptions

We assume that IEEE 802.11p beacon message broadcast works under the following scenarios. (1) A 2-D strip-like network area can be approximated to a 1-D single lane. (3) All nodes are treated as homogeneous with identical vehicle length L_V and transmission power P_t. (4) Mobile nodes are placed on the lines according to NHPP with the density of vehicles at a distance x from the tagged node: $\beta(x)$ (in nodes per meter). Then, the probability of finding i vehicles in a space interval $(x, x+l)$ is given by

$$P[i,(x,x+l)] = \frac{\left(\int_x^{x+l} \beta(y)dy\right)^i e^{-\int_x^{x+l} \beta(y)dy}}{i!}.$$

(5) Same *Nakagami* fading model is assumed for vehicular communication channel. (6) The distance between an interfere and the tagged transmitter should be no longer than $2r_E$ (Ni et al., 2015), where r_E is the average sensing range $r_E = d_0 \sqrt[\alpha]{P_t\eta/P_{th}}$, and P_{th} is the clear channel assessment(CCA) sensitivity. Then, PDF of the power P_r received from a receiver with distance d away from a source node is rewritten as

$$f_{P_r|d}(x) = \frac{1}{\Gamma(m)}\left(\frac{m}{\bar{P}_r(d)}\right)^m x^{m-1} \exp\left(-\frac{mx}{\bar{P}_r(d)}\right),$$

where $\Gamma()$ is the Gamma function, and m is the fading parameter. $\bar{P}_r(d) = P_t\eta\left(\frac{d_0}{d}\right)^\alpha$ (η is a transceiver-determined constant, d_0 is the reference distance for the far-zone field, α is the pathloss exponent) is the mean value determined by the pathloss.

3 ANALYSIS OF SINR DISTRIBUTION

As shown in Figure 1, given that there are l nodes in the shaded interference region, and the interfere I is the $(l-i)$-th node within the right shaded region $(i = 1, \ldots, l-1)$, Denote d_l be the distance between the tagged node T and the $l-th$ node (the farthest interfering node) within the right shaded region $[r_E, d_{max}]$ where dmax is the maximum range of all intended interfering nodes. Given NHPP distribution of distance between nodes, according to (Ma and Chen, 2008) and (Haenggi, 2005), the complimentary cumulative probability distribution $P(d_l > r)$ is given by the probability that there is at least one node in the range of $d_{max} - r$ divided by the probability that is at least a node in the range of d_{max}:

$$P(d_l > r) = \frac{1 - e^{-\int_r^{d_{\max}} \beta(y)dy}}{1 - e^{-\int_0^{d_{\max}} \beta(y)dy}},$$

Then, the cumulative distribution function (CDF) of distance $d_l (r_E < d_l < 2r_E)$ can be calculated as

$$F_{d_l}(\tau) = P(d_l < \tau) = \frac{e^{-\int_\tau^{2r_E} \beta(y)dy} - e^{-\int_0^{2r_E} \beta(y)dy}}{1 - e^{-\int_0^{2r_E} \beta(y)dy}},$$

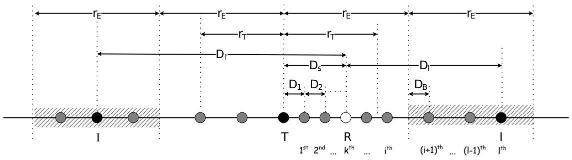

Figure 1: General interfering scenario for VANET safety message broadcast.

Since $d_{l-i} = d_{l-i+1} - Y_{l-i+1} (i = 1, \ldots, l-1)$, where Y_{l-i+1} is distance between $l-i+1$th node and $l-i$th node with distribution

$$F_{Y_{l-i+1}|d_{l-i+1}}(y|d) = 1 - e^{-\int_{d-y}^{d} \beta(z)dz},$$
$$f_{Y_{l-i+1}|d_{l-i+1}}(y|d) = \frac{dF_{Y_{l-i+1}|d_{l-i+1}}(y|d)}{dy} = \beta(d-y)e^{-\int_{d-y}^{d} \beta(z)dz}.$$

Consequently, the PDFs of distances of individual nodes $l-i$ in the shaded area can be derived as (Trivedi, 2002)

$$f_{l-i}(\tau) = \int_{\tau}^{2r_E} f_{l-i+1}(x) f_{Y_{l-i+1}|d_{l-i+1}}((x-\tau)|x)dx, \quad i = 1, \ldots, l-1.$$

Given D_S is the distance between T and R, the distance between $(l-i)$-th interfering node and node R is denoted as $D_I (i = 0, \ldots, l-1)$, where $r_E - D_s \leq D_I \leq 2r_E - D_s$.

$$F_{D_I|(d_s,l-i)}(x) = P(D_I < x | r_E - d_s \leq D_I \leq 2r_E - d_s) = \frac{F_{l-i}(d_s + x)}{\int_{r_E}^{2r_E} f_{l-i}(\tau)d\tau}, i = 0, \ldots, l-1.$$

The PDFs of the distances of the individual interfering nodes to the receiver R are obtained as

$$f_{D_I|(d_s,l-i)}(x) = \frac{f_{l-i}(d_s + x)}{\int_{r_E}^{2r_E} f_{l-i}(\tau)d\tau}, i = 0, \ldots, l-1. \quad (1)$$

From (1), the probability that there are l nodes in the shaded area is

$$P[l, (r_E, 2r_E)] = \frac{\left(\int_{r_E}^{2r_E} \beta(y)dy\right)^l e^{-\int_{r_E}^{2r_E} \beta(y)dy}}{l!}.$$

Then, the total D_I's conditional PDF can be expressed as

$$f_{D_I|d_s}(x) = \sum_{l=1}^{\infty} P[l, (r_E, 2r_E)] \sum_{j=0}^{l-1} f_{D_I|(d_s,l-j)}(x) p_j, \quad (2)$$

where p_j is the probability that the interfere I is the $j-th$ node within the right shaded area, which is evaluated as

$$p_j = 1/l, j = 0, 1, \ldots, l-1.$$

Similar to the derivation of D_I's PDF, D_S's PDF can be solved as follows. Assign $D_i i = 1, 2, \ldots,$ as distances of ith vehicle to the tagged vehicle T, then,

$$F_{D_1}(x) = 1 - e^{-\int_0^x \beta(z)dz}; f_{D_1}(x) = \beta x e^{-\int_0^x \beta(z)dz}.$$

Since $D_i = D_{i-1} - Y_{d_{i-1}} (i = 2, \ldots, l)$, where $Y_{d_{i-1}}$ is distance between $i-1$th node and ith $(i = 2, \ldots, l)$ node with distribution

$$F_{Y_{d_{i-1}}|d_{i-1}}(y|d) = 1 - e^{-\int_d^{d+y} \beta(z)dz},$$
$$f_{Y_{d_{i-1}}|d_{i-1}}(y|d) = \beta(d+y)e^{-\int_d^{d+y} \beta(z)dz},$$
$$f_{D_i}(\tau) = \int_0^{\tau} f_{D_{i-1}}(x) f_{Y_{d_{i-1}}|d_{l-1}}((\tau - x)|x)dx.$$

Then, the total D_S's PDF can be expressed as

$$f_{D_S}(x) = \sum_{l=1}^{\infty} P[l, (0, r_E)] \sum_{j=1}^{l} f_{D_j}(x) \frac{1}{l}.$$

The CDF of I's interference power P_I received at R could be presented as

$$F_{P_I|d_s}(x) = \Pr(P_I < x | D_S = d_s) = \int_{t'=0}^{x} \int_{r_E-d_s}^{2r_E-d_s} f_{P_r|D_I}(t') f_{D_I|d_s}(t) dt dt',$$
$$f_{P_I|d_s}(x) = \int_{r_E-d_s}^{2r_E-d_s} f_{P_r|D_I}(x) f_{D_I|d_s}(t) dt, \quad (3)$$

Next, we evaluate effect of transmissions from node I' at left hand side of T on R's reception. In similar way, CDF and PDF of I''s interference power at R can also be derived. Given D_S is the distance between T and R, the distance between $(l'-i)-th$ interfering node and node R is denoted as $D_{I'} (i = 0, \ldots, l'-1)$, where $r_E + D_s \leq D_{I'} \leq 2r_E + D_s$.

$$F_{D_{I'}|(d_s,l'-i)}(x) = P(D_{I'} < x | r_E + d_s \leq D_{I'} \leq 2r_E + d_s) = \frac{F_{l'-i}(x - d_s)}{\int_{r_E}^{2r_E} f_{l'-i}(\tau)d\tau}.$$

The PDFs of the distances of the individual interfering nodes to the receiver R are obtained as

$$f_{D_{I'}|(d_s,l'-i)}(x) = \frac{dF_{D_I(d_s,l'-i)}(x)}{dx} = \frac{f_{l'-i}(x - d_s)}{\int_{r_E}^{2r_E} f_{l'-i}(\tau)d\tau},$$
$$f_{D_{I'}|d_s}(x) = \sum_{l=1}^{\infty} P[l, (r_E, 2r_E)] \sum_{j=0}^{l-1} f_{D_{I'}|(d_s,l-j)}(x) p_j, \quad (4)$$
$$F_{P_{I'}|d_s}(x) = \Pr(P_{I'} < x | D_S = d_s) = \int_{t'=0}^{x} \int_{r_E+d_s}^{2r_E+d_s} f_{P_r|D_{I'}}(t') f_{D_{I'}|d_s}(t) dt dt',$$

$$f_{P_{I'}|d_s}(x) = \int_{r_E+d_s}^{2r_E+d_s} f_{P_r|D_{I'}}(x) f_{D_{I'}|d_s}(t)dt, \quad (5)$$

Therefore, the total interference power accumulated at the receiver R if the interferences from two sides occur at same time (Ni et al., 2015):

$$f_{P_{I+I'}|d_s}(x) = \int_0^\infty f_{P_I|d_s}(x-t) f_{P_{I'}|d_s}(t)dt,$$

Considering node T and node R are out of mutual carrier sensing range, T's transmission could occur at any time of T's transmission. According to (Yin et al., 2013), the probability that a node in the shaded area transmits during the vulnerable period of the transmission from the tagged node T is evaluated as

$$p_t = \pi_{XMT} \frac{2(T - DIFS)}{T},$$

where π_{XMT} is the steady-state probability that a vehicle is in transmission state, which is derived in (Yin et al., 2013). T is the time duration for one packet transmission, $DIFS$ is a time period of distributed inter-frame space of IEEE 802.11p MAC.

Hence, considering three possible interference occurrence cases from two sides of the receiver with different probabilities (single interferer from one side, and two interferers from both sides), the total interference power accumulated at the receiver R is the sum of two independent random variables from two sides of R.

At the same time, we should consider the distribution of interference power when there is no interference on both sides. In this case, the interference power is the power of the basic noise, which is assumed to be constant and expressed by P_{I_n}. The CDF and PDF of the interference power is:

$$F_{P_{I_n}|d_s}(x) = \begin{cases} 1, & if\ x \geq P_{I_n} \\ 0, & if\ x < P_{I_n}, \end{cases}$$

$$f_{P_{I_n}|d_s}(x) = dF_{P_{I_n}|d_s}(x)/dx. \quad (6)$$

Thus, PDF of interference power on R is expressed as

$$\begin{aligned} f_{P_\Sigma|d_s}(x) = & \left[1 - e^{-\Delta_R}\right]\left[1 - e^{-\Delta_L}\right] f_{P_{I+I'}|d_s}(x) \\ & + e^{-\Delta_L}\left[1 - e^{-\Delta_R}\right] f_{P_I|d_s}(x) \\ & + e^{-\Delta_R}\left[1 - e^{-\Delta_L}\right] f_{P_{I'}|d_s}(x) \\ & + e^{-\Delta_L} e^{-\Delta_R} f_{P_{I_n}|d_s}(x) \end{aligned}$$

where $\Delta_R = p_t \int_{r_E}^{2r_E} \beta(y)dy$; $\Delta_L = p_t \int_{-2r_E}^{-r_E} \beta(y)dy$.

Given $D_s = d_s$, the SINR at R is the ratio of two random variables, and its conditional PDF and CDF could be presented as

$$f_{SINR|d_s}(x) = \int_0^\infty t \cdot f_{P_r|d_s}(t \cdot x) f_{P_\Sigma|d_s}(t)dt,$$

$$F_{SINR|d_s}(x) = \int_0^x f_{SINR|d_s}(t)dt, x > 0,$$

Then, the SINR's PDF can be derived as

$$f_{SINR}(x) = \int_0^{r_E} f_{SINR|d_s}(x) f_{D_s}(t)dt,$$

$$F_{SINR}(x) = \int_0^x f_{SINR}(t)dt, x > 0.$$

4 QoS AND CAPACITY DERIVATION

Having derived SINR distribution, the following QoS metrics and capacity can be defined and evaluated.

4.1 QoS Derivation

First, the probability that receiver with distance ds to the tagged node accepts the message successfully if the measured conditional SINR is bigger than the given threshold and the received signal is stronger than the reception threshold P_{th}, which is expressed as

$$\begin{aligned} PRP(d_s, \theta) &= \Pr(SINR \geq \theta | d_s) \cdot \Pr(P_r \geq P_{th} | d_s) \\ &= (1 - F_{SINR|d_s}(\theta))(1 - \int_0^{P_{th}} f_{P_r|d_s}(x)dx), d_s \leq d_{ROI}. \end{aligned} \quad (7)$$

Define region of interest (ROI) of a safety application as size of the geographical region covered by those entities participating in the application, which is denoted as d_{ROI}. Different kinds of safety applications have different ROI sizes (Bai et al., 2006). Second, packet reception ratio (PRR) (the percentage of receivers that are free from transmission errors) within ROI can be evaluated as

$$PRR(d, \theta) = \frac{\int_0^d \beta(x) PRP(x, \theta)dx}{\int_0^d \beta(x)dx}, d \leq d_{ROI}.$$

4.2 Capacity Evaluation

The CDF of link capacity can be obtained from the Shannon's Theorem(Ni et al., 2015):

$$F_C(x) = \Pr(W \log_2(1 + SINR) < x) = F_{SINR}(2^{x/W} - 1),$$

where W is the bandwidth allocated to the observed communication pair. The PDF of link capacity is as follow:

$$f_C(x) = \frac{\ln 2}{W} \cdot (2^{x/W}) f_{SINR}(2^{x/W} - 1).$$

Then Expected link capacity is calculated according to the following formula:

$$E(C) = \int_0^\infty x f_C(x)dx.$$

5 ACCELERATION OF NUMERICAL COMPUTATION

5.1 Problem Description

Formula (7) of $PRP(d_s, \theta)$ can not be simplified, so it needs to be solved by numerical calculation.

The $F_{SINR|d_s}(x)$ and $F_{P_r|d_s}(x)$ need to be calculated for computing the PRP , in which the computational overhead of $F_{P_r|d_s}(x)$ can be neglected. Thus the formula mainly took in $F_{SINR|d_s}(x)$ calculation.

5.2 Influence of $f_{D_I|d_s}(x)$ and $f_{D_{I'}|d_s}(x)$ on Computational Efficiency

This section lists all the formulas involved in calculating $F_{SINR|d_s}(\theta)$:

$$F_{SINR|d_s}(\theta) = \int_0^\theta f_{SINR|d_s}(k)dk,$$

$$f_{SINR|d_s}(k) = \int_{\frac{P_{th}}{k}}^\infty t \cdot f_{P_r|d_s}(t \cdot k) \cdot \varphi_\Sigma(t, d_s)dt,$$

$$\begin{aligned}
\varphi_\Sigma(t, d_s) &= f_{P_\Sigma|d_s}(t) \\
&= [1-e^{-\Delta_R}][1-e^{-\Delta_L}] \int_0^\infty f_{P_I|d_s}(t-m) f_{P_{I'}|d_s}(m)dm \\
&+ e^{-\Delta_L}[1-e^{-\Delta_R}] f_{P_I|d_s}(t) \\
&+ e^{-\Delta_R}[1-e^{-\Delta_L}] f_{P_{I'}|d_s}(t) \\
&+ e^{-\Delta_L} e^{-\Delta_R} f_{P_{I_n}|d_s}(t).
\end{aligned}$$

Formula $f_{P_I|d_s}(x)$ and $f_{P_{I'}|d_s}(x)$ are shown in (3) and (5), respectively. In order to calculate formulas $f_{P_I|d_s}(x)$ and $f_{P_{I'}|d_s}(x)$, $f_{D_I|d_s}(x)$ and $f_{D_{I'}|d_s}(x)$ need to be calculated first, their expressions are shown in formulas (2) and (4).

Formulas (2) and (4) show that their computational time complexity is $O(n^2)$. If they are not simplified, it will cost a lot in the subsequent calculation process. Fortunately, by changing the summation order, the formulas can be reduced to the following forms, and their computational time complexity is reduced to $O(n)$:

$$f_{D_I|d_s}(x) = \sum_{l=0}^{n} f_{D_I|(d_s, l-l)}(x) \sum_{j=l+1}^{n+1} P[j-1, (r_E, 2r_E)] p_j, \quad p_j = 1/j \tag{8}$$

$$f_{D_{I'}|d_s}(x) = \sum_{l=0}^{n} f_{D_{I'}|(d_s, l-l)}(x) \sum_{j=l+1}^{n+1} P[j-1, (r_E, 2r_E)] p_j, \quad p_j = 1/j \tag{9}$$

Variable n is the upper limit of the number of vehicles in the communication range.

5.3 Implementation Scheme of MPI and Monte Carlo Method

5.3.1 Representation of Objective Function

For the convenience of description, we represent the following variables with c_1, c_2, c_3 :

$$\begin{aligned}
c_1 &= [1-e^{-\Delta_L}][1-e^{-\Delta_R}], \\
c_2 &= e^{-\Delta_L}[1-e^{-\Delta_R}], \\
c_3 &= e^{-\Delta_R}[1-e^{-\Delta_L}].
\end{aligned}$$

Let:

$$\begin{aligned}
f_1 = f_1(t,k) &= t \cdot f_{P_r|d_s}(t \cdot k), \\
f_2 = f_2(t,j) &= f_{P_r|D_I}(t) f_{D_I|d_s}(j), \\
f_3 = f_3(t,j) &= f_{P_r|D_{I'}}(t) f_{D_{I'}|d_s}(j).
\end{aligned}$$

Expanding the formula of $F_{SINR|d_s}(\theta)$, the formula (10) is obtained:

$$\begin{aligned}
F_{SINR|d_s}(\theta) &= \int_0^\theta f_{SINR|d_s}(k)dk \\
&= c_1 \int_0^\theta \int_{\frac{P_{th}}{k}}^\infty f_1 \int_0^\infty \Big(\int_{r_E-d_s}^{2r_E-d_s} f_2(t-m, j)dj \int_{r_E+d_s}^{2r_E+d_s} f_3(m,l)dl \Big) \\
& dmdtdk + c_2 \int_0^\theta \int_{\frac{P_{th}}{k}}^\infty f_1 \int_{r_E-d_s}^{2r_E-d_s} f_2 djdtdk \\
& + c_3 \int_0^\theta \int_{\frac{P_{th}}{k}}^\infty f_1 \int_{r_E+d_s}^{2r_E+d_s} f_3 djdtdk \\
& + e^{-\Delta_L} e^{-\Delta_R} \int_0^\theta \int_{\frac{P_{th}}{k}}^\infty t \cdot f_{P_r|d_s}(t \cdot k) \cdot f_{P_{I_n}|d_s}(t)dtdk.
\end{aligned} \tag{10}$$

Let, $F_{SINR|(d_s, P_{I_n})}(\theta) = \int_0^\theta \int_{\frac{P_{th}}{k}}^\infty t \cdot f_{P_r|d_s}(t \cdot k) \cdot f_{P_{I_n}|d_s}(t)dtdk$. Noise is the only source of interference at this time. Because its power P_{I_n} is assumed to be constant, so the value of the formula can be obtained by using the definition of $SINR$. Its calculation time is constant, so it is not considered in subsequent numerical calculation.

And use BI, RI, LI, NI to represent

$$c_1 \int_0^\theta \int_{\frac{P_{th}}{k}}^\infty f_1 \int_0^\infty \Big(\int_{r_E-d_s}^{2r_E-d_s} f_2(t-m, j)dj \int_{r_E+d_s}^{2r_E+d_s} f_3(m,l)dl \Big) dmdtdk,$$

$$c_2 \int_0^\theta \int_{\frac{P_{th}}{k}}^\infty f_1 \int_{r_E-d_s}^{2r_E-d_s} f_2 djdtdk,$$

$$c_3\int_0^{\theta}\int_{\frac{p_{th}}{k}}^{\infty} f_1 \int_{r_E+d_s}^{2r_E+d_s} f_3 d\,j dt dk,$$

$$e^{-\Delta_L}e^{-\Delta_R}\int_0^{\theta}\int_{\frac{p_{th}}{k}}^{\infty} t\cdot f_{P_r|d_s}(t\cdot k)\cdot f_{P_{In}|d_s}(t)dtdk.$$

After the transformation, as shown in Equation (11).

$$F_{SINR|d_s}(\theta) = BI + RI + LI + NI. \tag{11}$$

Formula (10) shows, that solving $F_{SINR|d_s}(\theta)$ need to calculate multidimensional integrals. The realizability and efficiency of numerical methods is a very important problem. The Monte Carlo integration method can calculate multidimensional integrals, and the integration speed is only related to the number of sampling points, and is independent of the dimension. So we use Monte Carlo integral to solve the multidimensional integral problem in this paper.

In order to speed up the solution, we use MPI to solve $PRP(d_s,\theta)$.

Figure 2 shows the process of dividing/calculating, synchronizing and reducing for the MPI. We use the process numbered 0 as the main process and use N processes to calculate $PRP(d_s,\theta)$. Figure 2 gives the flow of the entire program.

First, the main process calculates the parts that are independent of the integral function of the integral according to the input parameters, such as c_1, c_2, c_3, and the integral area volume v_1, v_2, v_3;

Secondly, according to the total Monte Carlo number of samples N, the mean values and the errors of the LI, BI and RI are calculated, respectively;

Finally, the main process calculates the value $PRP(d_s,\theta)$ based on the value of $F_{SINR|d_s}(\theta)$.

The detailed implementation is presented by pseudo code in Algorithm 1.

Algorithm 2 shows the process of MPI parallel coupled with Monte Carlo numerical method to estimate the mean $E(f;N)$ and the error $\sigma^2(E;N)$, by increasing sampling points to ensure the error $\sigma^2(E;N)$.

The detailed implementation is presented by pseudo code in Algorithm 2.

Algorithm 1: Scalable algorithm for VANET QoS analysis.

Require: QoS analysis problem, the total number of samples N of Monte Carlo , the number of MPI calculated processes k;
Ensure: Numerical solution, Monte Carlo error eps;
Detach QoS analysis problem into three part LI, RI, BI ;
Calculate the part that is independent of the integrands of the integral;
The number of samples to be calculated for each process is divided equally into N/k;
for each $subproblem \in LI, RI, BI$ **do**
    Use the k process call algorithm 2 to get the summation value sum;
    Accumulate the sum of these k processes and get the final summation value sum_final;
    Sum_final divided by N, get the mean of the integrands;
    The main process calculates the error eps and outputs it;
end for

Algorithm 2: Parallel algorithm of Monte Carlo method.

Require: The integrands function f, the total number of samples N of Monte Carlo , the number of MPI calculated processes k;
Ensure: The estimate of the integral $E(f;N)$, the error on this estimate $\sigma^2(E;N)$;
for $i = 1$ to k **do**
    Generate $\lceil N/k \rceil$ sampling points $\mathcal{P}_i$ by each process i;
    Compute $f(p_{i,j})$ for each sampling point $p_{i,j} \in \mathcal{P}_i$ sequentially in each parallel process i;
    Keep all result of $f(p_{i,j})$ in shared memory;
end for
Calculate the average $\hat{f}$ of $f(p_{i,j})$, $1 \le i \le k, 1 \le j \le \lceil N/k \rceil$;
Calculate the estimated integral $E(f;N) = V\hat{f}$ and estimated absolute error $\sigma^2(E;N) = \frac{N^2}{V^2}\sum_{i=1}^{k}\sum_{j=1}^{\lceil N/k \rceil}(f(p_{i,j})-\hat{f})^2$;

5.4 Experiments

We develop the experiments based on MPI cluster which include 20 cores CPU for numerical integration. The hardware of nodes in MPI cluster is Intel E5-2660 2.60GHz CPU and 32GB memory, and each node in cluster is organized by IntelMPI 5.1.2. Our developed numerical programs create one MPI process which is allocated 64MB local memory to compute for each core. The programs apply the GNU numerical computing library to generate random number and calculate integral, the seed of random numbers in each process should be different for various cycles. Parameters are set as follows:$SINR$ value θ is set as 4, and signal propagation distance d_s is set as 50. The average time of single sampling for LI,RI and BI is 105.07, 105.18 and 736462 ms, respectively. Due to the convolution, the sampling of BI spends thousands of times than LI, RI.

The experiments need large enough sampling points to ensure accuracy for Monte Carlo integration. Table 1 is the statistics of integration errors of LI, RI and BI parts under different number of sampling points to obtain QoS metric PRP. The number of sam-

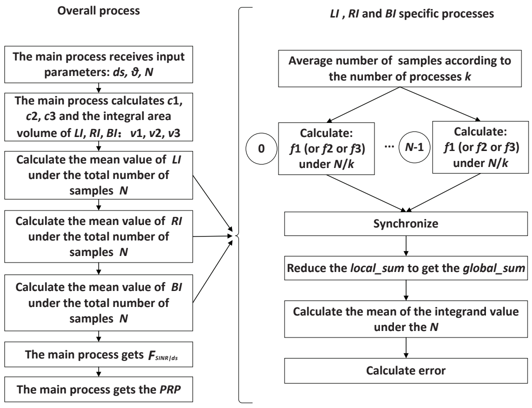

Figure 2: MPI program description.

pling points applied in our experiment is 1000, 3000 and 5000 times, respectively. The results in Table 1 is the average error of 7 times of evaluation. As shown in table 1, the estimated absolute error decreases as the number of sampling points N. However, more sampling means more computing resources.

Table 1: Integral error under different number of samples.

	LI	RI	BI
The error of 1000 sampling	1.49e-05	6.55e-05	1.38e-04
The error of 3000 sampling	8.02e-06	1.91e-05	3.41e-05
The error of 5000 sampling	8.47e-06	1.12e-05	2.13e-05

The total running time of the program under 1000, 3000 and 5000 samples is 20.08, 41.82 and 61.36 hours, respectively. The running time means the real time of program running in parallel by 20 cores. The process time increases significantly with the number of sampling, since it's important to trade off computing resources with evaluation accurracy when applied the model based on *SINR*. Thus, we employ the Monte Carlo integration with 3000 sampling points to compute various SINR settings.

6 COMPARISON OF THEORETICAL AND SIMULATION RESULTS

To validate the new proposed theoretical analysis, the Matlab and C++ are deployed for theoretical computations with MPI Monte Carlo method, and NS2 is deployed for network simulations. We consider a specific DSRC VANET in highway for safety message dissemination. Each vehicle in the network is equipped with DSRC capability. The communication network parameters as set as follows. $W = 10MHz$ (DSRC channel bandwidth), $P_t = 0.28183815Watts$ (transmission power of each node), $P_{th} = 2.28289e-11Watts$ (carrier sensing power strength or clear channel assessment sensitivity), $d_0 = 100meters$ (the reference distance for the far-zone), $\eta = 7.29e-10$, $P_{I_n} = -99dBm$, $r_E = 300m$ (average sensing range), $\sigma = 16s$ (Slot time), $DIFS = 64s$, $CW = 15$, $T_{H1} = 40s$ (PHY preamble), $T_{H2} = 272bits$ (MAC header), $T_{H3} = 4s$, (PLCP header), $T_c = 0.1s$ (Packet generation interval), $R_d = 24Mbps$ (Data rate), $PL = 200bytes$ (Packet length), $\alpha = 2$ (path loss exponent), Fading Parameter m for $r<50m$, $50m<r<150m$ and $r \geq 150m$, the value is 3, 1.5 and 1, respectively. The communication nodes are Poisson distributed with piecewise constant densities on highway with length of 1000m on each of the crossing roads.

The density distribution, as function of distances (X) to a tagged vehicle, in the case of $x \leq 50m$, $50m < x \leq 100m$ and $x > 100m$, is $3\beta_{av}/2$, β_{av} and $\beta_{av}/2$, respectively. where β_{av} is a constant average road density during a certain time period. Figure 3 and 4 shows the CDF and the PDF of SINR at the receivers with different values of the signal propagation distance d_s and SINR thresholds, respectively. β_{av}=0.1 vehicles/meter. It can be seen from Fig. 3, the farther propagation distance, the smaller received signal power, and accordingly the smaller SINR at receiver obtained. Thus, we can see the CDF's increasing trends with the propagation distance equaling with 50m, 250m, 350m and 450m, i.e., the SINR at the receiver with propagation distance 50m could be largest compared with the other propagation distance while the SINR at the receiver with 450m could be smallest. As with the Fig.3, it is also observed the PDFs varying trends with propagation distance with 50m, 250m, 350m and 450m in Fig. 4. It first increase with the propagation distance when SINR is relatively small and then decrease with SINR. The PDFs varying trends indicate that the closer the transmission distance is, the greater the SINR value at the receiving node has.

Figure 5 and 6 shows the *PRP* and *PRR* at the receivers with different values of the signal propagation distance d_s and SINR thresholds. It is shown from Figure 5 and 6 that analytical results practically coincide with the simulation results, which verify correctness of the proposed model. Both *PRP* and *PRR* with short propagation distance have better performance than that with long distance, i.e., the performance of *PRP* as well as *PRR* with propagation distance 50m is better than that of 150m, and the performance of *PRP* as well as *PRR* with 150m is better than that of 250m, and hence with 350m or 450m. On the other hand, it is observed that fixed propagation distance 50m, 150m, 250m and 350m, the performance of *PRP* as well as

PRR is decreasing with SINR thresholds, respectively. because the modulation and coding mechanism of the receiver could be better applied at the small SINR threshold, and thus the packet loss is smaller. Figure 7 shows link capacity of the local VANET . From figure 7 we can see that the range of link capacity is among $[78, 105]$ Mbps with high probability.

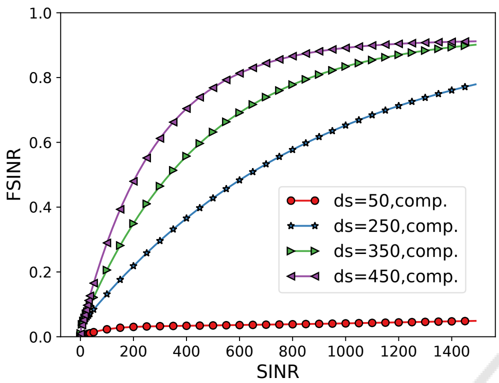

Figure 3: Conditional CDF of SINR at receiver.

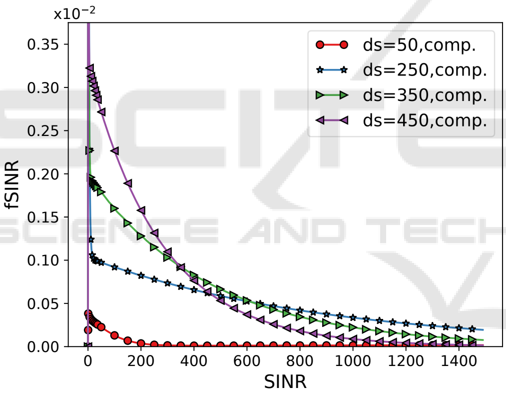

Figure 4: Conditional PDF of SINR at receiver.

7 CONCLUSION

In this paper, a start-of-the-art framework based on SINR for safety message broadcast are proposed, which is more practical and has the ability to analyze link capacity and reliability metrics of PRR and PRP. Assumptions such as NHPP vehicle distributions and Nakagami fading channel model with path loss make proposed model more practical and general. The detailed description about the assumptions and derivation of the SINR is in section 2 to 4. However, the model based on SINR introduces complex equation which spends significant computation resources to evaluate, Monte Carlo and MPI methods are proposed for accelerate computation process. At the end

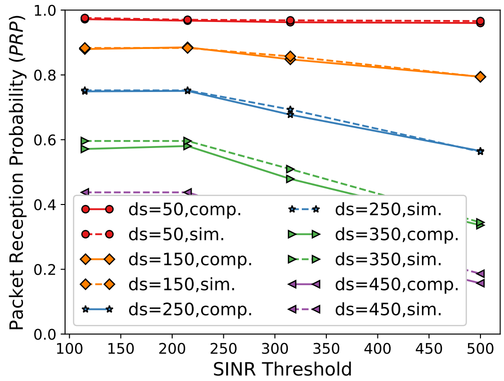

Figure 5: *PRP* of VANET with communication range.

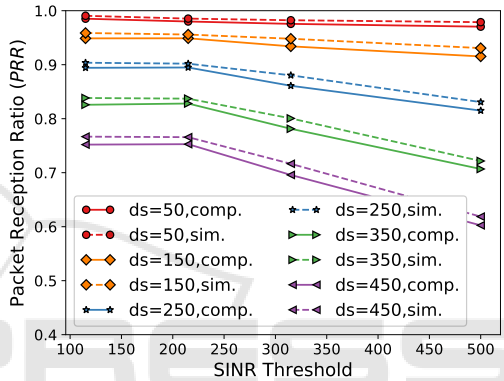

Figure 6: *PRR* of VANET with communication range.

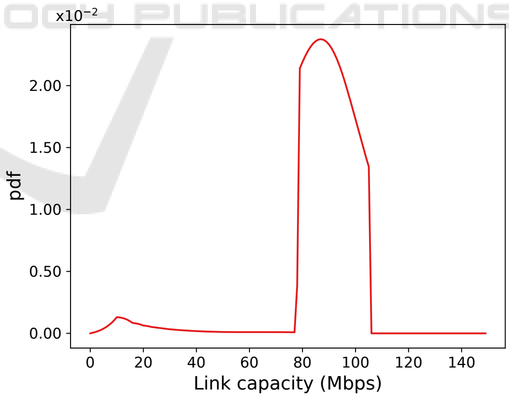

Figure 7: Link capacity of VANET broadcast.

of paper, we analyze the computation efforts and evaluation error of model by several experiments and validate its correctness by simulation. The analytical results give the numerical CDF and the PDF of SINR at the receivers with signal propagation distance d_s and SINR thresholds, respectively. The results could further be utilized by the engineer to measure the VANET communication system, and then optimize the system parameters which should be the future research direction. The analytical results of PRP and PRR practically coincide with the simulation results, which verify correctness of the proposed model.

ACKNOWLEDGEMENT

This work is supported by the National Nature Science Foundation of China under Grant 61572150, the Fundamental Research Funds for the Central Universities of DUT, No.DUT17RC(3)097.

REFERENCES

Andrisano, O., Verdone, R., and Nakagawa, M. (2000). Intelligent transportation systems: the role of third generation mobile radio networks. *IEEE Communications Magazine*, 38(9):144–151.

Arumugam, K., Godunov, A., Ranjan, D., Terzic, B., and Zubair, M. (2013). An efficient deterministic parallel algorithm for adaptive multidimensional numerical integration on gpus. In *2013 42nd International Conference on Parallel Processing*, pages 486–491. IEEE.

Bai, F., Elbatt, T., Hollan, G., Krishnan, H., and Sadekar, V. (2006). Towards characterizing and classifying communication-based automotive applications from a wireless networking perspective. In *Proceedings of IEEE Workshop on Automotive Networking and Applications (AutoNet)*, pages 1–25. San Francisco, CA, USA.

Bazzi, A., Campolo, C., Masini, B. M., Molinaro, A., Zanella, A., and Berthet, A. O. (2018). Enhancing cooperative driving in ieee 802.11 vehicular networks through full-duplex radios. *IEEE Transactions on Wireless Communications*, 17(4):2402–2416.

Bazzi, A., Cecchini, G., Menarini, M., Masini, B., and Zanella, A. (2019). Survey and perspectives of vehicular wi-fi versus sidelink cellular-v2x in the 5g era. *Future Internet*, 11:122.

Chen, Q., Schmidt-Eisenlohr, F., Jiang, D., Torrent-Moreno, M., Delgrossi, L., and Hartenstein, H. (2007). Overhaul of ieee 802.11 modeling and simulation in ns-2. In *Proceedings of the 10th ACM Symposium on Modeling, analysis, and simulation of wireless and mobile systems*, pages 159–168. ACM.

Eckermann, F., Kahlert, M., and Wietfeld, C. (2019). Performance analysis of c-v2x mode 4 communication introducing an open-source c-v2x simulator. *arXiv preprint arXiv:1907.09977*.

Gerstner, T. and Griebel, M. (1998). Numerical integration using sparse grids. *Numerical algorithms*, 18(3-4):209.

Gotsis, A., Maliatsos, K., Vasileiou, P., Stefanatos, S., Poulakis, M., and Alexiou, A. (2017). Experimenting with flexible d2d communications in current and future lte networks: A d2d radio technology primer & software modem implementation. In *2017 Wireless Innovation Forum European Conference on Communication Technologies and Software Defined Radio*. wirelessinnovation.

Gropp, W., Lusk, E., Doss, N., and Skjellum, A. (1996). A high-performance, portable implementation of the mpi message passing interface standard. *Parallel computing*, 22(6):789–828.

Gunter, T., Osborne, M. A., Garnett, R., Hennig, P., and Roberts, S. J. (2014). Sampling for inference in probabilistic models with fast bayesian quadrature. In *Advances in neural information processing systems*, pages 2789–2797.

Haenggi, M. (2005). On distances in uniformly random networks. *IEEE Transactions on Information Theory*, 51(10):3584–3586.

Hafeez, K. A., Zhao, L., Ma, B., and Mark, J. W. (2013). Performance analysis and enhancement of the DSRC for VANET's safety applications. *IEEE Transactions on Vehicular Technology*, 62(7):3069–3083.

Hassan, M. I., Vu, H. L., and Sakurai, T. (2011). Performance analysis of the IEEE 802.11 MAC protocol for DSRC safety applications. *IEEE Transactions on Vehicular Technology*, 60(8):3882–3896.

Lu, N. and Shen, X. S. (2014). *Capacity Analysis of Vehicular Communication Networks*. Springer.

Luong, H., Panda, M., Hai, V., and Bao, V. (2017). Analysis of multi-hop probabilistic forwarding for vehicular safety applications on highways. *IEEE Transactions on Mobile Computing*, 16(4):918–933.

Ma, X., Butron, G., and Trivedi, K. (2016). Modeling of vanet for bsm safety messaging at intersections with non-homogeneous node distribution. In *International Workshop on Communication Technologies for Vehicles*, pages 149–162. Springer.

Ma, X. and Chen, X. (2008). Performance analysis of ieee 802.11 broadcast scheme in ad hoc wireless lans. *IEEE Transactions on Vehicular Technology*, 57(6):3757–3768.

Ma, X., Lu, H., Zhao, J., Wang, Y., Li, J., and Ni, M. (2017). Comments on "interference-based capacity analysis of vehicular ad hoc networks". *IEEE Communications Letters*, 21(10):2322–2325.

Ma, X., Wilson, M., Yin, X., and Trivedi, K. S. (2013a). Performance of vanet safety message broadcast at rural intersections. In *2013 9th International Wireless Communications and Mobile Computing Conference (IWCMC)*, pages 1617–1622. IEEE.

Ma, X., Yin, X., Wilson, M., and Trivedi, K. S. (2013b). Mac and application-level broadcast reliability in vanets with channel fading. In *2013 international conference on computing, networking and communications (ICNC)*, pages 756–761. IEEE.

Ma, X., Zhang, J., and Wu, T. (2011). Reliability Analysis of One-Hop Safety-Critical Broadcast Services in VANETs. *IEEE Transactions on Vehicular Technology*, 60(8):3933–3946.

Ma, X., Zhao, J., Wang, Y., Zhang, T., and Li, Z. (2021). A new approach to sinr-based reliability analysis of ieee

802.11 broadcast ad hoc networks. *IEEE Communications Letters*, 25(2):651–655.

Molisch, A. F. (2012). *Wireless communications*, volume 34. John Wiley & Sons.

Morokoff, W. J. and Caflisch, R. E. (1995). Quasi-monte carlo integration. *Journal of computational physics*, 122(2):218–230.

Ni, M., Pan, J., Cai, L., Yu, J., Wu, H., and Zhong, Z. (2015). Interference-based capacity analysis for vehicular ad hoc networks. *IEEE Communications Letters*, 19(4):621–624.

Razak, F., Talip, M., Yakub, M., Khairudin, A., Izam, T., and Zaman, F. (2017). High speed numerical integration algorithm using fpga. *Journal of Fundamental and Applied Sciences*, 9(4S):131–144.

Schmidt-Eisenlohr, F. (2010). *Interference in vehicle-to-vehicle communication networks: Analysis, modeling, simulation and assessment*. KIT Scientific Publishing.

Shaban, A. M., Kurnaz, S., and Shantaf, A. M. (2020). Evaluation dsdv, aodv and olsr routing protocols in real live by using sumo with ns3 simulation in vanet. In *2020 International Congress on Human-Computer Interaction, Optimization and Robotic Applications (HORA)*, pages 1–5.

Steinmetz, E., Wildemeersch, M., Quek, T. Q., and Wymeersch, H. (2015). A stochastic geometry model for vehicular communication near intersections. In *2015 IEEE Globecom Workshops (GC Wkshps)*, pages 1–6. IEEE.

Tong, Z., Lu, H., Haenggi, M., and Poellabauer, C. (2016). A Stochastic Geometry Approach to the Modeling of DSRC for Vehicular Safety Communication. *IEEE Trans. Intelligent Transportation Systems*, 17(5):1448–1458.

Trivedi, K. S. (2002). *Probability and Statistics with Reliability, Queuing and Computer Science Applications*. John Wiley and Sons Ltd., Chichester, UK, 2nd edition edition.

Wang, M., Shan, H., Luan, T. H., Lu, N., and Bai, F. (2015). Asymptotic throughput capacity analysis of vanets exploiting mobility diversity. *IEEE Transactions on Vehicular Technology*, 64(9):4187–4202.

Yao, Y., Rao, L., and Liu, X. (2013). Performance and reliability analysis of IEEE 802.11 p safety communication in a highway environment. *IEEE Transactions on Vehicular Technology*, 62(9):4198–4212.

Yao, Y., Zhou, X., and Zhang, K. (2014). Density-aware rate adaptation for vehicle safety communications in the highway environment. *IEEE Communications Letters*, 18(7):1167–1170.

Ye, F., Yim, R., Roy, S., and Zhang, J. (2011). Efficiency and reliability of one-hop broadcasting in vehicular ad hoc networks. *IEEE Journal on Selected Areas in Communications*, 29(1):151–160.

Yin, X., Ma, X., and Trivedi, K. S. (2013). An interacting stochastic models approach for the performance evaluation of dsrc vehicular safety communication. *IEEE Transactions on Computers*, 62(5):873–885.

Zong, H., Hua, R., Zhao, J., and Cao, Z. (2019). Parallel monte carlo integration algorithm based on gpu. In *2019 IEEE 14th International Conference on Intelligent Systems and Knowledge Engineering (ISKE)*, pages 790–794.